Syntheses, Crystal Structures, and Physical Properties of Dinuclear Copper(I) and Tetranuclear Mixed-Valence Copper(I,II) Complexes with Hydroxylated Bipyridyl-Like Ligands

Xian-Ming Zhang,[a] Ming-Liang Tong,[a] Meng-Lian Gong,[a] Hung-Kay Lee,[b] Li Luo,[c] King-Fai Li,[d] Ye-Xiang Tong,[a] and Xiao-Ming Chen*[a]

Abstract: Four copper complexes with hydroxylated bipyridyl-like ligands, namely $[Cu_2(ophen)_2]$ (**1**), $[Cu_4(ophen)_4(tp)]$ (**2**), $[Cu_4(obpy)_4(tp)]$ (**3**), and $[Cu_4(obpy)_4(dpdc)]\cdot 2H_2O$ (**4**), (Hophen = 2-hydroxy-1,10-phenanthroline, Hobpy = 6-hydroxy-2,2′-bipyridine, tp = terephthalate, dpdc = diphenyl-4,4′-dicarboxylate) have been synthesized hydrothermally. X-ray single-crystal structural analyses of these complexes reveal that 1,10-phenanthroline (phen) or 2,2′-bipyridine (bpy) ligands are hydroxylated into ophen or obpy during the reaction, which provides structural evidence for the long-time argued Gillard mechanism. The dinuclear copper(I) complex **1** has three supramolecular isomers in the solid state, in which short copper – copper distances (2.66 – 2.68 Å) indicate weak metal – metal bonding interactions. Each of the mixed-valence copper(I,II) complexes **2** – **4** consists of a pair of $[Cu_2(ophen)_2]^+$ or $[Cu_2(obpy)_2]^+$ fragments bridged by a dicarboxylate ligand into a neutral tetranuclear dumbbell structure. Dinuclear **1** is an intermediate in the formation of **2** and can be converted into **2** in the presence of additional copper(II) salt and tp ligands under hydrothermal conditions. In addition to the ophen-centered $\pi \rightarrow \pi^*$ excited-state emission, **1** shows strong emissions at ambient temperature, which may be tentatively assigned as an admixture of copper-centered d → s,p and MLCT excited states.

Keywords: copper · mixed-valent compounds · hydroxylation · Gillard mechanism · structure elucidation

Introduction

Considerable emphasis has been placed on the investigation of copper(I) and mixed-valence copper(I,II) complexes because simple mononuclear copper(I) complexes with N-heterocyclic ligands, particularly derivatives of 2,2′-bipyridine (bpy) and 1,10-phenanthroline (phen), have unusual photophysical and electrochemical properties,[1, 2] and polynuclear copper(I) complexes have diverse luminescent properties.[3–5] Oxidation of one of the copper(I) centers in a polynuclear species can afford mixed-valence Cu^{I} – Cu^{II} complexes,[6] which are of particular interest in the rare cases when the mixed-valence state is delocalized.[7, 8]

On the other hand, there are a number of so-called "anomalies" of reactivity of N-heterocyclic complexes in aqueous solutions, in particular, bpy and phen complexes.[9] A quarter of a century ago, Gillard proposed a covalent hydrate mechanism for rationalizing the anomalous properties of these N-heterocyclic complexes (Scheme 1).[10] The key to the Gillard mechanism is that coordination of pyridine to a metal ion has an effect similar to quaternization and consequently activates the α-carbon atom of the pyridine to be attacked by a nucleophilic hydroxide ion to form a covalent hydrate (**CH**). Owing to a lack of structural evidence for the **CH** intermediate, the mechanism was debated for a long time.[11, 12] Recently, we described two mixed-valence copper(I,II) complexes with hydroxylated bpy and phen ligands[13] that provide structural evidence for the Gillard mechanism. As an extension of our previous work, we now report herein the

[a] Prof. X.-M. Chen, X.-M. Zhang, Dr. M.-L. Tong, Prof. M.-L. Gong, Prof. Y.-X. Tong
School of Chemistry and Chemical Engineering
Sun Yat-Sen University
Guangzhou 510275 (China)
Fax: (+86) 20-8411-2245
E-mail: cescxm@zsu.edu.cn

[b] Dr. H.-K. Lee
Department of Chemistry
The Chinese University of Hong Kong
Shatin, New Territories, Hong Kong (China)

[c] Dr. L. Luo
Department of Applied Physics
Guangdong University of Technology
Guangzhou 510090 (China)

[d] K.-F. Li
Department of Physics
Hong Kong Baptist University
Kowloon Tong, Hong Kong (China)

Supporting information for this article is available on the WWW under http://www.chemeurj.org or from the author.

  0947-6539/02/0814-3187 $ 20.00+.50/0

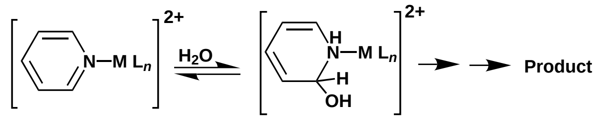

CH

Scheme 1. Schematic representation of the Gillard mechanism of covalent hydrate.

syntheses, crystal structures, and electrochemical and spectroscopic properties of a dinuclear copper(I) complex, namely $[Cu_2(ophen)_2]$ (**1**; Hophen = 2-hydroxy-1,10-phenanthroline) which has three supramolecular isomers, and three tetranuclear mixed-valence complexes, namely $[Cu_4(ophen)_4(tp)]$ (**2;** tp = terephthalate), $[Cu_4(obpy)_4(tp)]$ (**3**; Hobpy = 6-hydroxy-2,2′-bipyridine), and $[Cu_4(obpy)_4(dpdc)]\cdot 2H_2O$ (**4;** dpdc = diphenyl-4,4′-dicarboxylate).

Results and Discussion

Description of crystal structures: *The dinuclear copper(I) complex*: Dinuclear **1** crystallizes in three forms, the molecular structures of which are virtually identical. On the other hand, the three crystal forms show remarkable differences in terms of the molecular packing arrays, and thus are three supramolecular isomers. There is one crystallographically independent Cu^I atom in the α and β forms but two in the γ form (Figure 1). Each Cu^I atom in **1** adopts a trigonal

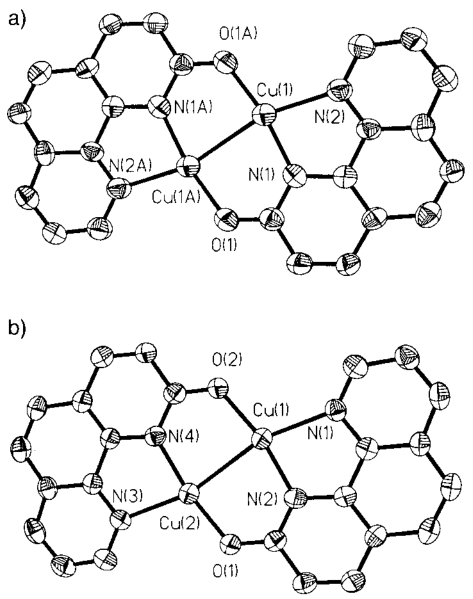

Figure 1. Structures of a) 1α or 1β, and b) 1γ (ORTEP plots with 35% thermal ellipsoids).

geometry, being coordinated by two nitrogen atoms from an ophen ligand and one oxygen atom from a deprotonated pyridyl hydroxy group of another ophen ligand. The Cu–O and Cu–N distances range from 1.916(5) to 1.923(5) Å and from 1.953(5) to 2.274(6) Å, respectively. The Cu–Cu distances in the α, β, and γ forms are 2.679(3), 2.661(2) and 2.673(2) Å, respectively, which are shorter than twice the van der Waals radius of Cu^I (2.8 Å) and are slightly longer than the Cu–Cu separation of 2.56 Å in metallic copper.[14] Weak bonding interactions have recently been proven in $[Cu_2(dcpm)_2]X_2$ (dcpm = bis(dicyclohexylphosphanyl)methane, X = ClO_4^-, PF_6^-) complexes which have short Cu^I–Cu^I distances of 2.64–2.93 Å.[15] Therefore, the Cu–Cu distance of 2.66–2.68 Å in **1** indicates similar Cu^I–Cu^I bonding interactions.

There are three types of supramolecular interactions in **1**, namely C–H···O hydrogen bonding, aromatic π–π stacking and intermolecular Cu···Cu interactions, which may be responsible for the existence of the three supramolecular isomers. In 1α, the C(11b)···O(1) distance is 3.432 Å and the ophen ligands between adjacent molecules are arranged in an off-set fashion with a plane-to-plane separation of 3.3–3.5 Å, indicating apparent C–H···O hydrogen bonds[16] and strong aromatic π–π stacking interactions.[17] Therefore, discrete molecules of 1α are extended into a two-dimensional (2D) supramolecular array in the solid (Figure 2). The Cu···Cu distance of 5.15 Å between two adjacent molecules indicates there is no intermolecular Cu···Cu interaction. In 1β, the C–H···O hydrogen bonds (C(6a)···O(1) 3.397 Å) link the discrete molecules into 2D arrays. Off-set aromatic π–π stacking interactions (separation 3.3–3.4 Å) and intermolecular Cu···Cu interactions (Cu···Cu 3.37 Å) in 1β further extend the 2D layers into a 3D array. Surprisingly, alternative intramolecular and intermolecular Cu···Cu interactions in 1β result in 1D zigzag metallic chains (see Figure S1 in the Supporting Information). In contrast to 1α and 1β, two discrete molecules in 1γ with intermolecular aromatic π–π interactions (plane-to-plane separation 3.1–3.3 Å) and Cu···Cu interactions (3.596 Å) are paired, and the molecular pairs are further connected by means of C–H···O hydrogen bonds (C(10a)···O(2) 3.435 Å) to generate a 3D supramolecular array.

Supramolecular isomerism lies at the heart of crystal engineering but, so far, known supramolecular isomers are very limited.[18] Therefore the structural characterization of three supramolecular isomers of **1** may provide structural data for calculating supramolecualar interactions.

Tetranuclear mixed-valence copper(I,II) complexes: Complexes **2**–**4** are structurally analogous since they all consist of a pair of $[Cu_2(ophen)_2]^+$ or $[Cu_2(obpy)_2]^+$ fragments bridged by a deprotonated dicarboxylate, μ_4-tp or μ_4-dpdc, into neutral tetranuclear dumbbell-shaped molecules, as depicted in Figures 3 and 4 (also see Figure 1 in reference [13]). Each of the two crystallographically independent copper atoms in **2**–**4** has a similar square-pyramidal coordination environment, being surrounded by a pair of nitrogen atoms (Cu–N 1.927(4)–2.099(5) Å) from an ophen or obpy, a deprotonated hydroxy group (Cu–O 1.913(3)–1.943(4) Å) from another ophen or obpy, and the adjacent copper atom (Cu–Cu 2.402(1)–2.443(2) Å) at the equatorial positions, and by a tp or dpdc carboxylate oxygen atom (Cu–O 2.167(5)–2.302(5) Å) at the apical position. These are consistent with most mixed-valence Cu_2^{3+} complexes documented previously,[7, 8, 19, 20] in which two metal atoms have

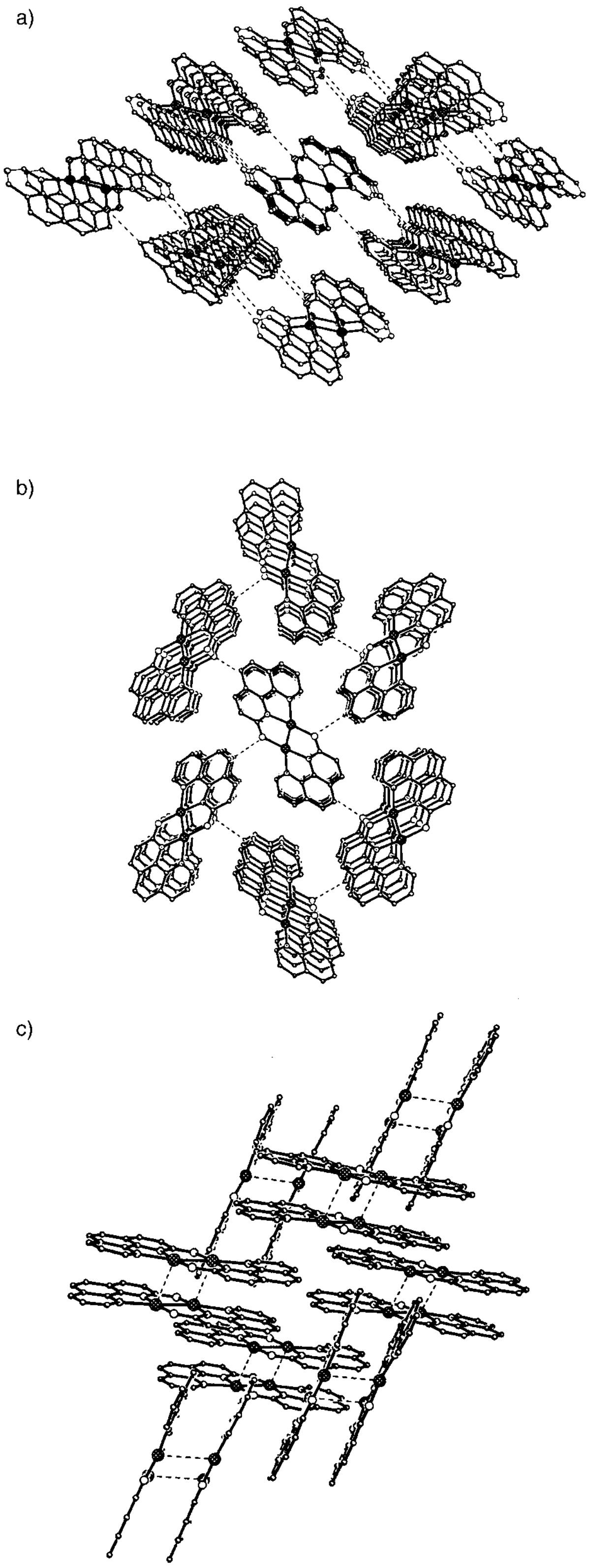

Figure 2. Perspective views of the stacking arrays of a) **1**α, b) **1**β, and c) **1**γ.

virtually identical coordination environments and form a short Cu–Cu bond with a bond order of 0.5. Bond valence sum (BVS) analyses also indicate that **2**–**4** are copper(1.5),copper(1.5) compounds.[21] The Cu^{I}–Cu^{II} bonding interactions in mixed-valence copper(I,II) complexes are important in metal-

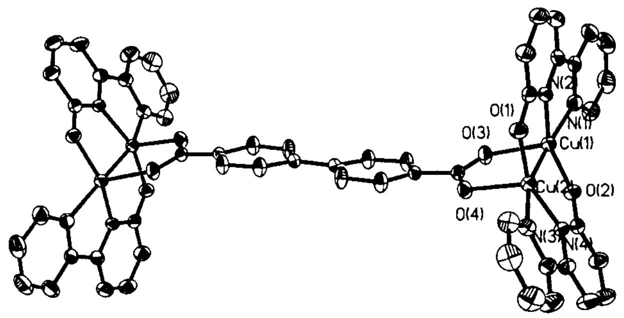

Figure 3. Structure of **4** (ORTEP plot with 35% thermal ellipsoids).

loprotein systems because they involve long-distance electron transfer.[22]

It should be noted that the $[Cu_2(ophen)_2]^+$ and $[Cu_2(obpy)_2]^+$ fragments in **2** and **3** are nearly coplanar but the $[Cu_2(obpy)_2]^+$ fragments in **4** are not; the dihedral angle between the two obpy ligands is 150°. Although the molecular structures of **2**–**4** are similar, their supramolecular arrays in the solid are quite different (see Figure 4). Compounds **2** and **3** display van der Waals interactions between intermolecular Cu_2^{3+} dimers as well as aromatic stacking interactions. Two Cu_2^{3+} dimers from neighboring molecules are arranged into a parallelogram with a diagonal side of 3.74 Å and a longer side of 4.05 Å in **2**, and into a rectangle with a longer side of 4.02 Å in **3**. In addition, the adjacent aromatic rings of ophen and obpy are stacked in an off-set fashion with a plane-to-plane separation of 3.4–3.8 Å in **2** and **3**. Thus, the intermolecular Cu$\cdots$Cu interactions and aromatic stacking interactions extend the molecules of **2** and **3** into 1D chains which are further extended by C–H$\cdots$O hydrogen bonds between the aromatic groups and carboxy groups from adjacent chains (C$\cdots$O 3.41–3.48 Å) into 3D supramolecular arrays (see Figure S2 and S3 in the Supporting Information). In contrast to **2** and **3**, there are no intermolecular Cu$\cdots$Cu and aromatic π–π stacking interactions in **4** due to the cross arrangement of the molecules in the solid, and the 3D supramolecular array is mainly held together by significant C–H$\cdots$O hydrogen bonds (C$\cdots$O 3.37–3.49 Å) (see Figure S4 in the Supporting Information). It is noteworthy that, in **2** and **3**, only carboxylate oxygen atoms are utilized as acceptors in the formation of C–H$\cdots$O hydrogen bonds, whereas in **4** both carboxylate and pyridyl hydroxy oxygen atoms are utilized as acceptors. This is the reason why the supramolecular array of **4** shows great differences from those of **2** and **3**.

Synthesis: Whilst a well-established method for the synthesis of zeolites, the hydrothermal method has more recently been adopted in the preparation of coordination complexes. In principle, this reaction exploits the self-assembly of soluble precursors and results in products that are similar to those formed by nucleation in solution.[23] However, the reduced viscosity of water in the hydrothermal temperature range of 120–240°C enhances the diffusion process and thus extraction of solids and crystal growth from solution are favored. Since the problem of differential solubility is minimized, a number of organic and inorganic components can be introduced for which the appropriate size and shape may be

  0947-6539/02/0814-3189 $ 20.00+.50/0

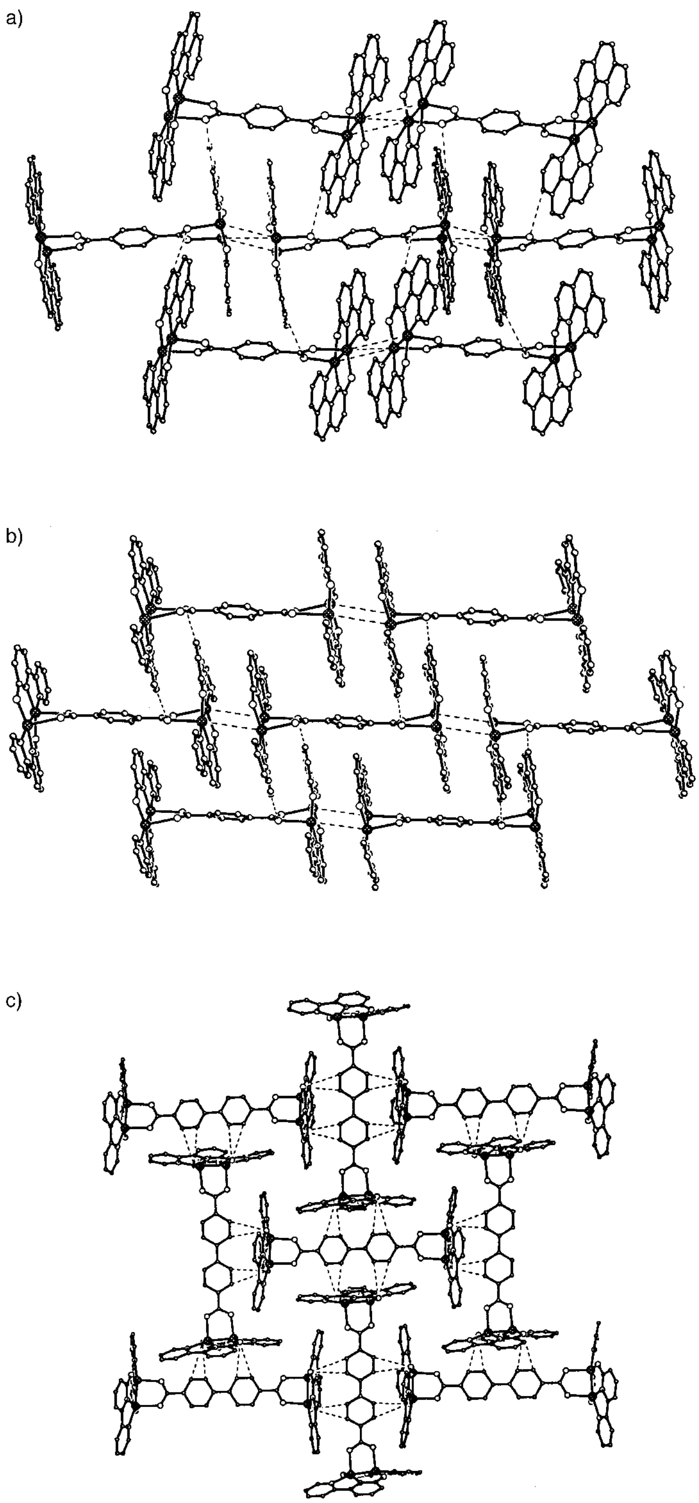

Figure 4. Views of the supramolecular layers of a) **2**, b) **3**, and c) **4**.

selected for efficient crystal packing during the crystallization process. Crystallization under hydrothermal conditions follows a non-equilibrium course, and thus a metastable phase may be preferentially isolated. After considering several pathways, the most stable phase can be isolated. There are a number of parameters to consider in hydrothermal reactions, such as time, temperature, pH value, and molar ratio of reactants; small changes in one or more of these parameters can have a profound influence on the final outcome of the reaction.

Complexes **1**–**4** were hydrothermally synthesized in the temperature range 140—185 °C under autogenous pressure with a filling volume of about 50 %. Complex **1** forms three supramolecular isomers in the solid state, and the preparation temperatures of the three isomers from low to high are in the sequence **1**γ, **1**α, and **1**β (Figure 2). The molecular symmetry from low to high follows the same sequence. These observations are consistent with an entropic effect; from the entropic point of view, a reaction at a higher temperature favors the formation of a structure with higher symmetry. In addition, complex **1** can be converted into mixed-valence tetranuclear **2** by addition of extra Cu^{II} salt and tp, and further hydrothermal treatment. Therefore, it may be regarded as the intermediate for the formation of **2**. The pH values in the preparations of **1**–**4** are weakly basic (8–9), which favor nucleophilic attack of hydroxide ions towards phen or bpy ligands to generate ophen or obpy.

Reaction mechanism: Hydroxylation of bpy and phen to produce Hobpy and Hophen observed in **1**–**4** is consistent with the formation of covalent hydrates in the Gillard mechanism and thus provides structural evidence for the mechanism. In addition, we found that the formation of **1**–**4** shows pH dependence (higher pH favoring the formation of **1**–**4**) which also indicates nucleophilic attack by a hydroxide ion on the coordinated bpy or phen during the reaction. In accord with the Gillard mechanism and other well-known organic reactions, the main steps towards dinuclear copper(I) and tetranuclear delocalized mixed-valence copper(I,II) complexes are proposed in Scheme 2. First, bpy or phen ligands are coordinated to copper(II) ions to form $[Cu(bpy)L_2]^{2+}$ or $[Cu(phen)L_2]^{2+}$ species. This step is the prerequisite for nucleophilic attack by hydroxide ions since the α-carbon atom of pyridine can only be activated by coordination of the bpy or phen to a Cu^{II} ion. Second, the α-carbon atom of pyridine is attacked by a nucleophilic hydroxide to form a mononuclear covalent hydrate (**CH**); the core step of the Gillard mechanism. Third, the deprotonation of mononulear covalent hydrate results in a pseudo-base (**PB**) species. The direct attack by a hydroxide ion to form a **PB** is equivalent to the addition of a water molecule to form a covalent hydrate followed by removal of a proton under basic condition. Fourth, two mononuclear **PB** species are dimerized to form a dinuclear **PB** species. Fifth, intramolecular electron transfer and dehydrogenation of the dinuclear **PB** species result in a neutral dinuclear copper(I) species. In this step, the role of the Cu^{II} ions as oxidant is critical in the fixation of the hydroxy group on the pyridyl ring. Sixth, intramolecular electron transfer again generates **1**. Finally, one-electron oxidization of the neutral dinuclear copper(I) molecule and dimerization of two dinuclear species by coordination of a tp bridge generate a molecule of **2**, concomitant with contraction of the Cu–Cu distance. In the formation course of **2**, a small amount of deep dark block crystals of **1**α was recovered as a by-product, which encouraged us to investigate **1** as the intermediate in the formation of **2**. Keeping all hydrothermal parameters unchanged except for the reaction time, the yield ratio of **2**:**1**α

0947-6539/02/0814-3190 $ 20.00+.50/0 *Chem. Eur. J.* **2002**, *8*, No. 14

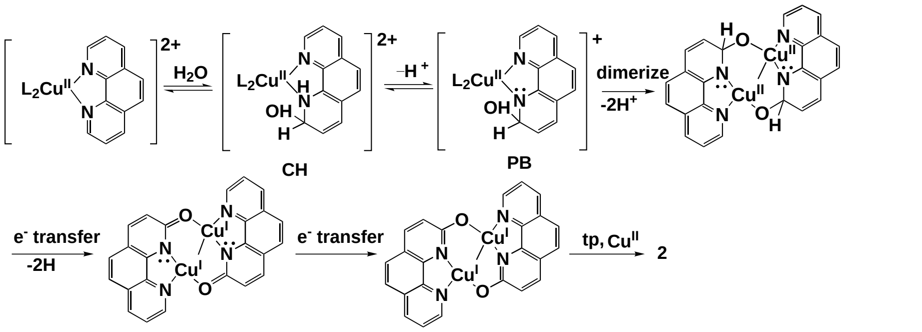

Scheme 2. The proposed formation mechanism of **2**.

signal as originating from copper(II) centers. One possible reason for the absence of the hyperfine lines is related to the low antibonding π* level of ophen and obpy ligands. Thus, we cannot categorize **2**–**4** as class II or class III mixed-valence systems.

increases with the extension of reaction time, indicating that **2** is the more stable phase. An analogous reaction of a mixture of **1** (in any form of the crystal isomers), $Cu(NO_3)_2$, H_2tp, and NaOH indeed yielded platelike dark brown crystals of **2**, which proves unambiguously that **1** is an intermediate during the formation of **2**. The proposed final step is supported by several reported examples of one-electron oxidation of dinuclear copper(I) center to prepare mixed-valence dinuclear copper(I,II) complexes. In particular, Lippard and co-workers prepared a series of delocalized mixed-valence complexes from dinuclear copper(I) intermediates by one-electron oxidation with silver salts.[19] The conversion of the dinuclear **1** to tetranuclear **2** was performed under a dinitrogen atmosphere, and thus the oxidant may possibly be the extra copper(II) ions in the reaction system. It should be pointed out that unstable covalent hydrate species can form from a $[CuL_2(phen)]^{2+}$ complex in any aqueous solution, however the successful isolation of hydroxylated bpy and phen ligands in this work is attributed to the fact that the coordinated Cu^{II} ions can act as an oxidant under hydrothermal conditions, hence resulting in the fixation of the hydroxy group.

Copper(II) salts are widely used as catalysts in oxidation reactions of alcohols to ketones or aldehydes, but in most cases the precise mechanisms are not clear and the intermediates have not fully been characterized.[24] The formation of copper(I) and mixed-valence copper(I,II) complexes involves the coordination of an hydroxyl group to the copper(II) ion, removal of the α-hydrogen atom and intramolecular electron transfer, which are known steps in the catalytic oxidation of alcohols to aldehydes or ketones by a copper(II) salt. Therefore, the formation mechanism of **1**–**4** is also helpful to understand the precise catalytic mechanism.

Magnetic properties: The mixed-valence states of the copper ions in **2**–**4** were also proven by the temperature-dependent magnetic susceptibility of **2** (Figure 5). An effective magnetic moment of 1.73 μ_B per Cu_2 unit at 200 K is consistent with one unpaired electron per dimer.

Although our investigations based on X-ray structural data, valence bond sum and magnetic susceptibility indicate that **2**, **3**, and **4** are averaged mixed-valence complexes, we failed to obtain the seven-line hyperfine splitting pattern[19] in solution EPR spectrocopy. However, the powdered EPR spectrum (see Figure S5 in the Supporting Information) shows a signal with nearly isotropic g factors ($g = 2.10$), which confirms the

Cyclic voltammetry: The cyclic voltammogram (CV) of **1** displays one reduction peak and three oxidation peaks (Figure 6a). The I_p at -0.675 V is roughly equal to twice of that at -0.533 or -0.271 V. Thus, we assign the reduction peak at -0.675 V to the two-electron reaction $[Cu^ICu^I(ophen)_2]^0 + 2e \rightarrow [Cu^0Cu^0(ophen)_2]^{2-}$. The oxidation peaks at -0.533 V and -0.271 V correspond to the two one-electron reactions $[Cu^0Cu^0(ophen)_2]^{2-} - e \rightarrow [Cu^ICu^0(ophen)_2]^-$ and $[Cu^ICu^0(ophen)_2]^- - e \rightarrow [Cu^ICu^I(ophen)_2]^0$, respectively. In addition, another irreversible oxidation peak at 0.519 V corresponds to the reaction of $[Cu^ICu^I(ophen)_2] - 2e \rightarrow [Cu^{II}Cu^{II}(ophen)_2]^{2+}$, corresponding to the decomposition of **1** and is consistent with the fact that copper(II) ions having three coordinate atoms are usually unstable.[25] The CV of **2** displays two reversible couples (Figure 6b). The redox couple with the reduction peak at -1.346 V and oxidation peak at -1.332 V corresponds to the reaction $[Cu_2^ICu_2^{II}(ophen)_4(tp)] + 2e \leftrightarrow [Cu_4^I(ophen)_4(tp)]^{2-}$. The other couple with reduction peak at -0.054 V and oxidation peak at 0.028 V can be assigned to the reaction $[Cu_4^{II}(ophen)_4(tp)]^{2+} + 2e \leftrightarrow [Cu_2^ICu_2^{II}(ophen)_4(tp)]$. This observation suggests that **2** is more easily oxidized than other relevant mixed-valence Cu(I,II) complexes.[19]

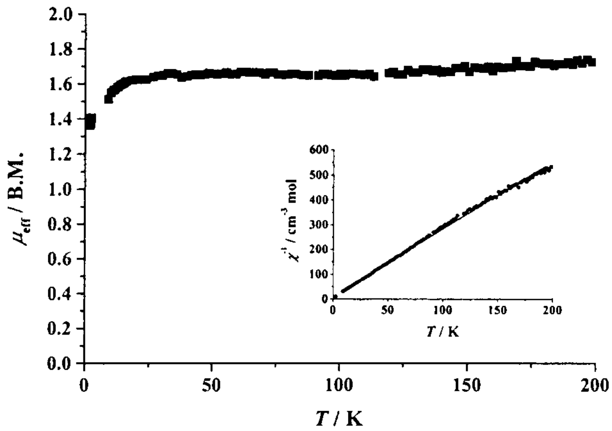

Figure 5. Temperature-dependent magnetic susceptibility of **2** at 10 kOe. Plot of μ_{eff} versus T; inset: plot of χ^{-1} versus T.

The electrochemical behaviors of **1** and **2** show great differences (Figure 6), possibly due to the difference in their coordination environments. The observations for **1** and **2** suggest that a single ophen ligand is not sufficient to stabilize the mixed-valence copper complex but an additional tp ligand is of great help in the stabilization of **2** in the range of -1.33–0 V.

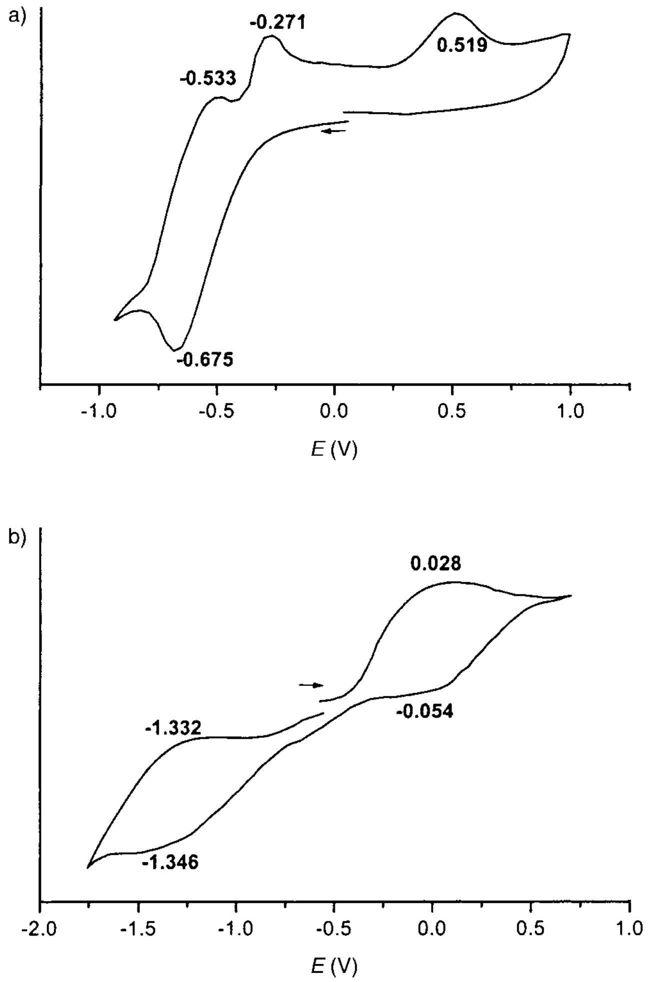

Figure 6. Cyclic voltammograms of a) **1** and b) **2** in DMF solution, scan rate 400 mV s^{-1}, potentials measured versus SCE.

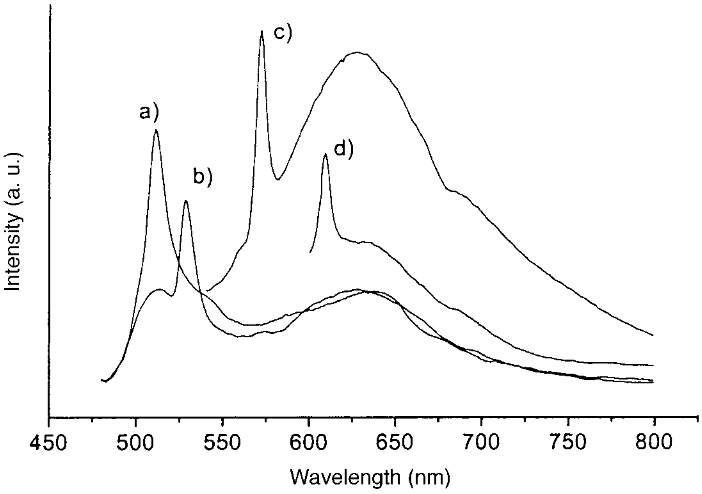

Figure 7. Photoluminescence spectra of **1** in DMF solution. Excitation wavelength [nm]: a) 422, b) 454, c) 488, d) 514.

Absorption and photoluminescence spectra: The absorption and photoluminescence spectra of the three isomers of **1** in DMF solution are identical, indicating that the different forms of **1** have the same solution structure. The UV/Vis absorption spectra of **1** consist of a sharp and intense absorption band at 288 nm and a broad absorption band centered at 352 nm. The former corresponds to $\pi \rightarrow \pi^*$ transition of the ophen ligand and the latter to $n \rightarrow \pi^*$ transition of the ophen ligand. Possibly, the MLCT absorption bands overlap with the latter one.

The photoluminescence spectrum of **1** in DMF solution shows a broad band centered at 425 nm upon excitation at 345 nm attributed to the ophen-centered $\pi \rightarrow \pi^*$ excited state (see Figure S6 in the Supporting Information). Besides the ligand-centered $\pi \rightarrow \pi^*$ excited-state transition, **1** also exhibits interesting diverse photoluminescent properties in weakly-coordinating DMF solution at room temperature (Figure 7). Upon excitation at 422 nm, the emission spectrum of **1** exhibits two broad bands (that apparent at 630 nm, $\tau = 4.9$ ns and the less apparent one at ca. 510 nm) and one narrow, strong band (511 nm; Figure 7a). Upon excitation at 454 nm, the emission maxima of the two broad bands at 511 and 630 nm remain unchanged but a narrow band appears at 526 nm (Figure 7b). Upon excitation at 488 and 514 nm, a narrow band appears at 575 ($\tau = 5$ ns) and 609 nm ($\tau = 5.4$ ns), respectively (Figure 7c). As mentioned above, two general trends are apparent in the luminescent properties of **1**. Upon excitation in the range of 420–514 nm, the emission maxima of the two broad bands do not change with the change of excitation wavelength but the emission maximum of the narrow band is red-shifted with the increase of excitation wavelength. Although luminescence of MLCT excited states of mononuclear copper(I) compounds of bis-1,10-phenanthroline has been extensively studied since the 1980s,[1][2] luminescence of polynuclear copper(I) complexes with chalcogenides, acetylides, multi-phosphanes, halides, and thiolates has received much attention recently.[15] Luminescence of polynuclear luminescent Cu^I complexes with α-hydroxylated pyridyl-type ligands has not been reported to date. Thus, only possible assignments for the excited states are given here and further exploration of related complexes and precise theoretical calculations are required before exact assignments can be made. Although from an energy point of view the broad band emission at 511 nm from the $n \rightarrow \pi^*$ excited state is favored, the assignment can be argued because **2** is not photoluminescent around 511 nm in both the solid state and solution. The Cu^I ion has a tendency to be oxidized and the ophen ligand possesses low-energy empty π^* orbitals. Thus, the broad-band emissions at 511 and 630 nm may result from the copper(I)-to-ophen charge transfer (MLCT). Luminescence of polynuclear d^{10} complexes supported by weak metal–metal interactions has been observed, and in view of the short Cu $\cdots$ Cu distance (ca. 2.68 Å) and the richness of emissions observed for **1**, an admixture of a metal-centered $d \rightarrow s,p$ excited state into the MLCT excited state is also possible. In fact, the admixture of different excited states including metal/XLCT and metal/LMCT has been reported in some polynuclear d^{10} luminescent complexes.[5] The lifetimes of these narrow bands at 511, 526, 575, and 609 nm are similar, and thus it may be reasonable to assign them to the same emission origin. As for the red shift of the narrow band with the red shift of excitation wavelength, it may be the result of populated energy levels which each match different excitation energies.

Conclusion

Four polynuclear copper(I) or copper(I,II) complexes containing copper(I)–copper(I) or copper(I)–copper(II) bonds were synthesized and structurally characterized. The hydroxylation of phen and bpy ligands leading to 2-hydroxy-1,10-phenanthroline and 6-hydroxy-2,2′-bipyridine in these polynuclear complexes provides structural support for the Gillard mechanism. The formation mechanisms of **1**–**4** involve electron transfer from the hydroxy oxygen atom to the Cu^{II} ion which is helpful in the understanding of the precise mechanism of catalytic oxidation of alcohol by a copper(II) salt. Dinuclear **1** is an intermediate in the synthesis of **2** and can be converted into **2** in the presence of extra copper(II) salt and tp ligands under hydrothermal conditions. Three supramolecular isomers of **1** represent a very rare case in crystal engineering, and also show rich photoluminescent properties.

Experimental Section

Preparations:

[Cu_2(ophen)$_2$] (1α): A mixture of $Cu(NO_3)_2 \cdot 3H_2O$ (0.120 g), phen (0.117 g), and water (10 mL) in a molar ratio of 1:1.3:1100 was stirred and adjusted to pH 8 with 2 M NaOH solution, then sealed in a 23-mL Teflon reactor and heated at 160 °C for 120 h. After cooling, deep dark block crystals of **1**α were filtered and dried in air (yield 35 %). Elemental analysis calcd (%) for $C_{24}H_{14}Cu_2N_4O_2$ (517.47): C 55.70, H 2.73, N 10.83; found: C 55.56, H 2.78, N 10.79; IR (KBr): $\tilde{\nu} = 3403$ m, 1621 m, 1585 s, 1517 s, 1428 s, 1138 m, 837 m, 732 w cm^{-1}.

[Cu_2(ophen)$_2$] (1β): A mixture of $Cu(NO_3)_2 \cdot 3H_2O$ (0.120 g), phen (0.09 g), and water (10 mL) in a molar ratio of 1:1:1100 was stirred and adjusted to pH 8.5 with 2 M NaOH solution, then sealed in a 23-mL Teflon reactor and heated at 175 °C for 120 h. After cooling, dark block crystals of **1**β were filtered and dried in air (yield 30 %). Elemental analysis calcd (%) for $C_{24}H_{14}Cu_2N_4O_2$ (517.47): C 55.70, H 2.73, N 10.83; found: C 55.75, H 2.70, N 10.91; IR (KBr): $\tilde{\nu} = 3403$ m, 1620 m, 1584 s, 1517 s, 1427 s, 1137 m, 837 m, 732 w cm^{-1}.

[Cu_2(ophen)$_2$] (1γ): A mixture of $Cu(NO_3)_2 \cdot 3H_2O$ (0.120 g), phen (0.162 g) and water (10 mL) in a molar ratio of 1:1.7:1100 was stirred and adjusted to pH 8 with 2 M NaOH solution, then sealed in a 23-mL Teflon reactor and heated at 150 °C for 120 h. Dark block crystals were filtered and dried in air (yield 45 %). Elemental analysis calcd(%) for $C_{24}H_{14}Cu_2N_4O_2$ (517.47): C 55.70, H 2.73, N 10.83; found: C 55.64, H 2.76, N 10.92; IR data (KBr): $\tilde{\nu} = 3402$ m, 1619 s, 1586 s, 1516 s, 1427 s, 1138 m, 837 m, 731 w cm^{-1}.

[Cu_4(ophen)$_4$(tp)] (2): a) A mixture of $Cu(NO_3)_2 \cdot 3H_2O$ (0.120 g), phen (0.117 g), H_2tp (0.041 g), NaOH (0.02 g), and water (10 mL) in a molar ratio of 1:1.3:0.25:0.5:1100 was stirred for 20 min in air, then sealed in a 23-mL Teflon reactor and heated at 160 °C for 144 h. After cooling, dark brown platelike crystals of **2** (50 %) and dark block crystals of **1**α (3 %) were recovered. b) A mixture of **1** (0.103 g) (in any one crystal form), $Cu(NO_3)_2$ (0.047 g), H_2tp (0.017 g), NaOH (0.008 g) and water (4 mL) in a molar ratio of 1:1:0.5:1:1100 was sealed in a 23-mL Teflon reactor and heated at 160 °C for 72 h. Dark platelike crystals of **2** were recovered. Elemental analysis calcd (%) for $C_{28}H_{16}Cu_2N_4O_4$ (599.53): C 56.09, H 2.69, N 9.34; found: C 55.89, H 2.73, N 9.22; IR (KBr): $\tilde{\nu} = 3440$ m, 3050 w, 1622 m, 1563 s, 1511 s, 1485 s, 1459 s, 1386 s, 1365 s, 1142 m, 843 m, 734 m, 653 m cm^{-1}.

[Cu_4(obpy)$_4$(tp)] (3): A mixture of $Cu(NO_3)_2 \cdot 3H_2O$ (0.120 g), bpy (0.102 g), H_2tp (0.041 g), NaOH (0.02 g), and water (10 mL) in a molar ratio of 1:1.3:0.25:0.5:1100 was stirred for 20 min in air, then sealed in a 23-mL Teflon reactor and heated at 160 °C for 144 h. After cooling, dark brown platelike crystals of **3** were filtered and dried in air (yield 30 %). Elemental analysis calcd (%) for $C_{24}H_{16}Cu_2N_4O_4$ (551.49): C 52.27, H 2.92, N 10.16; found: C 52.16, H 2.88, N 10.03; IR (KBr): $\tilde{\nu} = 3433$ m, 3070 w, 1601 s, 1568 s, 1492 s, 1458 s, 1164 m, 1013 s, 812 m, 776 s, 746 m, 589 w cm^{-1}.

[Cu_4(obpy)$_4$(dpdc)] · $2H_2O$ (4): A mixture of $Cu(NO_3)_2 \cdot 3H_2O$ (0.120 g), bpy (0.122 g), H_2dpdc (0.061 g), NaOH (0.02 g), and water (10 mL) in a molar ratio of 1:1.6:0.25:0.5:1100 was stirred for 20 min in air, then sealed in a 23-mL Teflon reactor and heated at 185 °C and held for 164 h. After cooling, dark brown needlelike crystals were filtered and dried in air (yield 30 %). Elemental analysis calcd (%) for $C_{54}H_{40}Cu_4N_8O_{10}$ (1215.10): C 53.38, H 3.32, N 9.22; found: C 53.42, H 3.36, N 9.28; IR (KBr): $\tilde{\nu} = 3422$ m, 3067 w, 1596 s, 1565 s, 1488 s, 1455 s, 1159 m, 1011 s, 771 s, 584 w cm^{-1}.

Physical measurements: Elemental analyses were performed on a Perkin–Elmer 240 elemental analyzer. The FTIR spectra were recorded from KBr pellets in the range 400–4000 cm^{-1} on a Nicolet 5DX spectrometer. Magnetic susceptibility measurements in the 2–200 K temperature range were performed on a Maglab System[2000] magnetometer. Owing to the limited solubility of **1** and **2** in DMF, their saturated solutions were used in cyclic voltammetry and photoluminescent experiments. All potentials quoted are versus SCE. The reversibility of the redox couples was judged against the usual criteria. The X-band EPR spectrum of **2** was recorded with a Bruker EMX spectrometer. The absorption spectra were recorded with a Perkin-Elmer 5 spectrometer. For the photoluminescence measurement, He-Cd or Ar-ion laser was used as the excitation source with the maximum power of 5 mW. The emission light of the samples was collected and detected by a 25 cm focal length double monochromator (Oriel 77225). For lifetime measurements, the third harmonics, 355 nm line of a Nd:YAG laser was used as excitation light.

Crystal structure determination: Diffraction intensities were collected at 293 K on a Siemens R3m diffractometer (for **1**α, **1**β, **1**γ, **2** and **3**) and a Bruker Smart 1000CCD diffractometer (for **4**) ($Mo_{K\alpha}$, $\lambda = 0.71073$ Å). Lorentz polarization and absorption corrections were applied. The structures were solved by direct methods (SHELXS-97)[26] and refined by using full-matrix least-squares technique (SHELXL-97).[27] Analytical expressions of neutral-atom scattering factors were employed, and anomalous dispersion corrections were incorporated. In all cases, all non-hydrogen atoms were refined anistropically and hydrogen atoms of organic ligands were geometrically placed. The crystallographic data for the six complexes are listed in Table 1 and the selected interatomic distances and

Table 1. Crystal and structure refinement for complexes **1**–**4**.

	1α	**1**β	**1**γ	**2**	**3**	**4**
empirical formula	$C_{24}H_{14}Cu_2N_4O_2$	$C_{24}H_{14}Cu_2N_4O_2$	$C_{24}H_{14}Cu_2N_4O_2$	$C_{28}H_{16}Cu_2N_4O_4$	$C_{24}H_{16}Cu_2N_4O_4$	$C_{54}H_{40}Cu_4N_8O_{10}$
formula weight	517.47	517.47	517.47	599.53	551.49	1215.10
crystal system	monoclinic	monoclinic	monoclinic	monoclinic	triclinic	monoclinic
space group	$P2_1/n$	$P2_1/n$	$P2_1/n$	$P2_1/n$	$P\bar{1}$	$P2_1/n$
a [Å]	10.651(8)	4.816(2)	11.982(12)	10.465(8)	10.047(8)	9.193(2)
b [Å]	6.180(4)	12.881(10)	11.164(10)	15.279(8)	10.668(7)	17.502(4)
c [Å]	15.079(13)	15.712(11)	14.829(14)	15.425(12)	11.186(7)	15.123(3)
α [°]					79.550(10)	
β [°]	94.160(10)	95.25(13)	97.16(2)	104.60(15)	71.76(16)	90.16(3)
γ [°]					69.940(10)	
V [Å^3]	989.9(13)	970.6(11)	1968(3)	2387(3)	1065.9(13)	2433.2(9)
Z	2	2	4	4	2	2
R_{int}	0.0846	0.0414	0.0486	0.0567	0.0636	0.0343
R_1 [$I > 2\sigma(I)$]	0.0731	0.0500	0.0538	0.0609	0.0667	0.0502
wR_2	0.2275	0.1458	0.1356	0.1736	0.2101	0.1326

  0947-6539/02/0814-3193 $ 20.00+.50/0

angles are given in Table S1 in the Supporting Information. CCDC-170016, CCDC-170017, and CCDC-179611 to CCDC-179614 contain the supplementary crystallographic data (excluding structure factors) for the structure reported in this paper. These data can be can be obtained free of charge via www.ccdc.cam.ac.uk/conts/retrieving.html (or from the Cambridge Crystallographic Data Centre, 12 Union Road, Cambridge CB2 1EZ, UK; fax: (+44) 1223-336033; or deposit@ccdc.cam.ac.uk).

Acknowledgements

This work was supported by the National Natural Science Foundation of China (No. 20131020, 20001008 & 29971033) and the Ministry of Education of China (No. 01134).

[1] a) N. Armaroli, *Chem. Soc. Rev.* **2001**, *30*, 113; b) D. V. Scaltrito, D. W. Thompson, J. A. O'Callaghan, G. J. Meyer, *Coord. Chem. Rev.* **2000**, *208*, 243; c) D. R. McMillin, K. M. McNett, *Chem. Rev.* **1998**, *98*, 1201; d) D. G. Cuttell, S.-M. Kuang, P. E. Fanwick, D. R. McMillin, R. A. Walton, *J. Am. Chem. Soc.* **2002**, *124*, 6.

[2] a) D. Felder, J.-F. Nierengarten, F. Barigelletti, B. Ventura, N. Armaroli, *J. Am. Chem. Soc.* **2001**, *123*, 6291; b) D. A. Bardwell, A. M. W. Cargill Thompson, J. C. Jeffery, E. E. M. Tilley, M. D. Ward, *J. Chem. Soc. Dalton Trans.* **1995**, 835; c) P. Comba, T. W. Hambley, P. Hilfenhaus, D. T. Richens, *J. Chem. Soc. Dalton Trans.* **1996**, 533.

[3] a) K. M. Merz, Jr., R. Hoffmann, *Inorg. Chem.* **1988**, *27*, 2120; b) F. A. Cotton, X. Feng, M. Matusz, R. Poli, *J. Am. Chem. Soc.* **1988**, *110,* 7077; P. C. Ford, *Coord. Chem. Rev.* **1994**, *132*, 129; c) E. Cariati, J. Bourassa, P. C. Ford, *Chem. Commun.* **1998**, 1623; d) V. W. W. Yam, W. K. Lee, T. F. Lai, *J. Chem. Soc. Chem. Commun.* **1993**, 1571.

[4] P. C. Ford, A. Vogler, *Acc. Chem. Res.* **1993**, *26*, 220.

[5] V. W. W. Yam and K. K. W. Lo, *Chem. Soc. Rev.* **1999**, *28*, 323.

[6] M. Dunaj-Jurco, G. Ondrejovic, M. Melnik, *Coord. Chem. Rev.* **1988**, *83*, 1.

[7] a) C. Harding, V. McKee, J. Nelson, *J. Am. Chem. Soc.* **1991**, *11*3, 9684; b) M. E. Barr, P. H. Smith, W. E. Antholine, B. Spencer, *J. Chem. Soc. Chem. Commun.* **1993**, 1649; c) C. Harding, J. Nelson, M. C. R. Symons, J. Wyatt, *J. Chem. Soc. Chem. Commun.* **1994**, 2499; d) R. P. Houser, V. G., Young, Jr., W. B. Tolman, *J. Am. Chem. Soc.* **1996**, *118*, 2101.

[8] a) J. A. Halfen, S. Mahapatra, E. C. Wilkinson, A. J. Gengenbach, V. G. Young, Jr., L. Que, Jr., W. B. Tolman, *J. Am. Chem. Soc.* **1996**, *118*, 763; b) R. P. Houser, W. B. Tolman, *Inorg. Chem.* **1995**, *34*, 1632; c) F. Neese, W. G. Zumft, W. E. Antholine, P. M. H. Kroneck, *J. Am. Chem. Soc.* **1996**, *118*, 8692; d) T. D. Westmoreland, D. E. Wilcox, M. J. Baldwin, W. B. Mims, E. I. Solomon, *J. Am. Chem. Soc.* **1989**, *111*, 6106.

[9] a) J. Burgess, *J. Chem. Soc. Dalton Trans.* **1972**, 1061; b) D. W. Margerum, *J. Am. Chem. Soc.* **1957**, *79*, 2728; c) F. P. Dwyer, E. C. Gyarfas, *J. Am. Chem. Soc.* **1954**, *76*, 6320; d) R. D. Gillard, R. E. E. Hill, *J. Chem. Soc. Dalton Trans.* **1974**, 1217.

[10] R. D. Gillard, *Coord. Chem. Rev.* **1975**, *16*, 67.

[11] a) M. S. Henry, M. Z. Hoffman, *J. Am. Chem. Soc.* **1977**, *99*, 5201; b) A. Gameiro, R. D. Gillard, M. M. R. Bakhsh, N. H. Rees, *Chem. Commun.* **1996**, 2245.

[12] a) N. Serpone, G. Ponterini, M. A. Jamieson, *Coord. Chem. Rev.* **1983**, *50*, 209; b) W. A. Wickramasinghe, P. H. Bird, M. A. Jamieson, N. Serpone, *J. Chem. Soc. Chem. Commun.* **1979**, 798; c) O. Farver, O. Monsted, G. Nord, *J. Am. Chem. Soc.* **1979**, *101*, 6118; d) D. Dandrini, M. T. Gandolfi, L. Moggi, V. Balzani, *J. Am. Chem. Soc.* **1978**, *100*, 1463; E. C. Constable, *Polyhedron* **1983**, *2*, 551.

[13] X.-M. Zhang, M.-L. Tong, X.-M. Chen, *Angew. Chem.* **2002**, 114, 1071; *Angew. Chem. Int. Ed.* **2002**, *41*, 1029.

[14] P. L. Jones, J. C. Jeffery, J. P. Maher, J. A. McCleverty, P. H. Rieger, M. D. Ward, *Inorg. Chem.* **1997**, *36,* 3088.

[15] C. M. Che, Z. Mao, V. M. Miskowski, M. C. Tse, C. K. Chan, K. K. Cheung, D. L. Philips, K. H. Leung, *Angew. Chem.* **2000**, *112*, 4250; *Angew. Chem. Int. Ed.* **2000**, *39*, 4084.

[16] G. R. Desiraju, *Acc. Chem. Res.* **1996**, *29*, 441.

[17] C. Janiak, *J. Chem. Soc. Dalton Trans.* **2000**, 3885.

[18] B. Moulton, M. J. Zaworotko, *Chem. Rev.* **2001**, *101*, 1629.

[19] D. D. LeCloux, R. Davydov, S. J. Lippard, *J. Am. Chem. Soc.* **1998**, *120*, 6810.

[20] S. M.-F. Lo, S. S.-Y. Chui, L.-Y. Shek, Z.-Y. Lin, X.-X. Zhang, G.-H. Wen, I. D. Williams, *J. Am. Chem. Soc.* **2000**, *122*, 6293.

[21] T. B. Zunic, I. Vickovic, IVTON - Program for the Calculation of Geometrical Aspects of Crystal Structures and Some Crystal Chemical Applications *J. Appl. Crystallogr.* **1996**, *29*, 305. Charges of copper atoms were calculated and results show that charges for Cu(1) and Cu(2) in **2** are 1.51 and 1.51.

[22] G. Al-Obaidi Baranovic, J. Coyle, C. G. Coates, J. J. McGarvey, V. McKee, J. Nelson, *Inorg. Chem.* **1998**, *37*, 3567.

[23] R. M. Barrer, *Hydrothermal Chemistry of Zeolites*, Academic Press, London, **1982**.

[24] E. C. Constable, *Metals and Ligand Reactivity,* VCH, Weinheim, **1996**.

[25] P. L. Holland, W. B. Tolman, *J. Am. Chem. Soc.* **1999**, *121*, 7270.

[26] G. M. Sheldrick, SHELXS-97, Program for Crystal Structure Solution, Göttingen University, Germany, **1997**.

[27] G. M. Sheldrick, SHELXL-97, Program for Crystal Structure Refinement, Göttingen University, Germany, **1997**.

Received: February 21, 2002 [F3892]

